

Membrane undulations near a plane rigid surface

Oded Farago¹

¹Department of Biomedical Engineering, Ben Gurion University, Be'er Sheva 84105, Israel

We use analytical calculations and Monte Carlo simulations to determine the thermal undulation spectrum of a membrane patch of a few tens of nanometer in size, whose corners are located at a fixed distance d above a plane rigid surface. Our analysis shows that the surface influence on the bilayer undulations can be effectively described in terms of a uniform conning potential that grows quadratically with the height of the membrane h relative to the surface: $V = (1/2) \kappa h^2$. The strength of the harmonic conning potential vanishes when the corners of the membrane patch are placed directly on the surface ($d = 0$), and achieves its maximum value when d is of the order of a few nanometers. However, even at maximum strength the conning effect is quite small and has noticeable impact only on the amplitude of the largest bending mode.

PACS numbers:

I. INTRODUCTION

Fatty acids and other lipids are essential to every living organism. Because of their amphiphilic nature, they spontaneously self-assemble into bilayer membranes that define the limits of cells and serve as permeability barrier to prevent proteins, ions and metabolites from leaking out of the cell and unwanted toxins leaking in [1]. In eukaryotic cells, membranes also surround the organelles allowing for organization of biological processes through compartmentalization. In addition, biological membranes host numerous proteins that are crucial for the mechanical stability of the cell, and which carry out a variety of functions such as energy and signal transduction, communication, and cellular homeostasis [2].

An important aspect of biological membranes is that they are typically not free but rather coned by other surrounding membranes, adhere to other membranes, and attach to elastic networks like the cytoskeleton and the extracellular matrix. Several model systems with reduced compositional complexity have been designed to mimic biological membranes. These biomimetic systems include phospholipid bilayers deposited onto solid substrates (solid-supported membranes) [3], or on ultra-thin polymer supports (polymer-supported membranes) [4]. With the aid of biochemical tools and generic engineering, supported membranes can be functionalized with various membrane-associated proteins [5]. Synthetic supported membranes with reconstituted proteins are increasingly used as controlled idealized models for studying key properties of cellular membranes [6]. They provide a natural environment for the immobilization of proteins under non-denaturing conditions and in well-defined orientation [7]. Another attractive application of supported membranes is the design of phantom cells exhibiting well-defined adhesive properties and receptor densities [8]. Finally, biofunctional membranes supported by solid interfaces (semiconductors, metals, plastics) provide new classes of biosensors, diagnostic tools, and other biocompatible materials [5, 9].

Theoretically, the thermal shape undulations of supported membranes have been addressed for various model systems. These model systems include: (i) membranes that adhere to surfaces under the action of a continuum local potential [10, 11], (ii) membranes pinned or tethered discretely to a surface [12, 13, 14, 15], and (iii) membranes supported by elastic networks of springs [16, 17, 18, 19, 20]. The investigation of the latter case is largely motivated by recent studies of simple cells (e.g., red blood cells and the lateral cortex of auditory outer hair cells), where the supporting cytoskeleton has a fairly well-defined connectivity [21]. One feature, missing in many previous theoretical studies, is the influence of steric ("excluded volume" -EV) interactions between the membrane and its support on the elasticity and shape undulations of the membrane. When these interactions are considered (see, e.g., refs. [11, 22]), it is usually assumed that the disjoining potential due to the collisions between the membrane and the underlying surface decreases inverse-quadratically with the distance between them. This result has been originally obtained in a heuristic manner by Helfrich [23], and later was formulated more systematically by using a renormalization-group approach and computer simulations (see [24] and refs. therein). An instructive way to understand this result is as follows: Consider a membrane that spans a planar square frame of area L^2 . The Helfrich energy (to quadratic order) for a nearly-flat membrane in the Monge gauge is given by

$$H = \frac{\kappa}{2} \int_0^L \int_0^L r^2 h^2 d^2 \mathbf{r}; \quad (1)$$

where κ the bending rigidity, and h the height of the membrane above the frame reference plane. Dividing the frame area into $\ell_0^2 = (L/\ell)^2$ grid cells of microscopic area ℓ^2 (where ℓ is of the order of the thickness of the bilayer), and

introducing the Fourier transform of $h(\mathbf{r})$

$$h_{\mathbf{q}} = \frac{1}{L^2} \int d^2\mathbf{r} h(\mathbf{r}) e^{i\mathbf{q}\cdot\mathbf{r}}; \quad \mathbf{q} = \frac{2\pi}{L} (n_1; n_2); \quad n_1, n_2 = \frac{L}{2L}; \dots; \frac{L}{2L}; \quad (2)$$

the Helfrich energy takes the form

$$H = \frac{L^4}{L^2} \sum_{\mathbf{q}} \frac{1}{2} q^4 h_{\mathbf{q}}^2; \quad (3)$$

from which (by invoking the equipartition theorem) one finds that

$$\langle h_{\mathbf{q}}^2 \rangle = \frac{k_B T L^2}{L^4 q^4}; \quad (4)$$

where k_B is Boltzmann factor, T the temperature, and $q = |\mathbf{q}| = (2\pi/L) (n_1^2 + n_2^2)^{1/2} = (2\pi/L)n$. Using the last result, one readily finds that the mean-square fluctuation of the height increases quadratically with L

$$\langle h^2 \rangle = \langle h(\mathbf{r})^2 \rangle = \frac{1}{L^4} \sum_{\mathbf{q}} \langle h_{\mathbf{q}}^2 \rangle = \frac{k_B T}{L^4} \sum_{\mathbf{q}} \frac{L^2}{q^4} = \frac{1}{n^4}, \quad \frac{6.03 k_B T}{(2\pi)^4} L^2; \quad (5)$$

Now, consider a membrane placed between two parallel walls positioned a distance d from each other, as shown schematically in Fig. 1. The presence of the walls significantly suppresses the long wavelength thermal fluctuations of the confined membrane. At large length scales, we may assume that the net result of the confinement is that the membrane experiences an effective harmonic potential which can be introduced as an additional term in the Helfrich Hamiltonian:

$$H = \int d^2\mathbf{r} \left[\frac{1}{2} \kappa (\nabla^2 h)^2 + \frac{1}{2} h^2 \right]; \quad (6)$$

where κ is a constant which will be determined later, and h is measured from the mid-plane between the walls. In Fourier space the energy reads

$$H = \frac{L^4}{L^2} \sum_{\mathbf{q}} \left[\frac{1}{2} q^4 + \frac{1}{2} \right] h_{\mathbf{q}}^2; \quad (7)$$

and the spectrum of fluctuations is given by

$$\langle h_{\mathbf{q}}^2 \rangle = \frac{k_B T L^2}{L^4 (q^4 + 1)}; \quad (8)$$

If $(2\pi/L)^4$ (which is always satisfied for sufficiently large L), then the mean-square fluctuation of the height is given by

$$\langle h^2 \rangle = \langle h(\mathbf{r})^2 \rangle = \frac{1}{L^4} \sum_{\mathbf{q}} \langle h_{\mathbf{q}}^2 \rangle = \frac{k_B T}{2\pi^2 d^4}; \quad (9)$$

This result can be used for determining the value of κ . Each point of the membrane has equal probability to be found anywhere between the walls. Therefore,

$$\langle h^2 \rangle = \frac{d^2}{12}; \quad (10)$$

and by comparing Eqs. (9) and (10), we find that

$$\kappa = \frac{36 (k_B T)^2}{2\pi^2 d^4}; \quad (11)$$

Due to the thermal fluctuations, the membrane collides with the confining walls and loses configurational entropy in these collisions. The walls will therefore experience a disjoining potential. Tracing over \mathbf{h}_q in Eq.(7) leads to the following expression for the Helmholtz free energy

$$F = \frac{k_B T}{2} \sum_q \ln \left[\frac{L^4 q^4 + \kappa^2}{2 L^2 k_B T} \right]; \quad (12)$$

where κ is the thermal de-Broglie wavelength of a microscopic membrane patch of area L^2 . The disjoining pressure between the walls is then calculated by using Eqs. (8) & (12) as follows:

$$p = -\frac{1}{L^2} \frac{\partial F}{\partial d} = -\frac{1}{L^2} \frac{\partial F}{\partial \kappa} \frac{\partial \kappa}{\partial d} = -\frac{\partial}{\partial d} \frac{\kappa^2}{2} = \frac{6 (k_B T)^2}{2 d^3}; \quad (13)$$

From this result it follows that the effective disjoining potential per unit area [25]:

$$V = \int_0^d p(x) dx = \frac{3 (k_B T)^2}{2 d^2}; \quad (14)$$

decays quadratically with d .

II. MEMBRANE FLUCTUATIONS NEAR A SINGLE PLANE SURFACE

Eq.(14) for the disjoining potential has been derived for the case of a membrane fluctuating between two walls. Does this result also hold in the case of a membrane fluctuating near a single rigid wall? Consider a square membrane of linear size L with bending rigidity κ whose four corners are held a distance d above a flat, impenetrable, surface (Fig. 2). The height of the membrane relative to the underlying surface is denoted by the function $h(x; y)$. In what follows, we shall assume that $h(x; y)$ is periodic (with period L) along both x and y directions. The pressure due to the collisions between the fluctuating membrane and the surface must be repulsive. However, it is not a priori obvious why p should be proportional to d^{-3} , as predicted by Eq.(13). Moreover, it is not even intuitively clear whether this pressure should enhance or suppress the amplitude of the membrane thermal fluctuations. The pinning of the edges of the membrane and the EV interactions with the surface represent a combination of attractive and repulsive potentials whose net effect is not really well understood. A better understanding of this issue can be obtained by comparing the configurational phase space of our model system membrane with that of a freely fluctuating membrane. In the free membrane case, we consider the ensemble of configurations for which the spatial average of the height, $\bar{h} = (1/L^2) \int h(x; y) dx dy$, is equal to some fixed arbitrary value c . Setting $\bar{h} = c$ is necessary to avoid multiple counting of physically equivalent configurations invariant under a vertical translation along the z direction. (Note the difference in notation between the spatial average \bar{h} ($= 1/L^2 \int h(x; y) dx dy$) which is calculated for a specific configuration, and $\langle h \rangle$ which is the statistical mechanical average over the ensemble of all possible (distinct) configurations.) The phase space of free membrane configurations can be further divided into sub-spaces, where the height functions h_1 and h_2 of each two configurations included in the same sub-space can be related by $h_1(x; y) = h_2(x + a; y + b)$ with $0 < a; b < L$. In other words, all the configurations in each sub-space can be transformed into each other by a horizontal translation in the $x-y$ plane (see Fig.3). This transformation does not change \bar{h} and, therefore, does not exclude (introduce) allowed (forbidden) configurations from (into) the phase space of configurations with $\bar{h} = c$. Since the Helfrich energy [Eq.(1)] is invariant under translations, all the configurations within each sub-space have exactly the same statistical weight. The partition function which involves summing over all possible configurations can be presented as summation over the "sub-spaces":

$$Z = \sum_{\text{con. gurations}} e^{-\frac{H}{k_B T}} = \sum_{\text{sub spaces}} e^{-\frac{H}{k_B T}} = \sum_{\text{sub spaces}} e^{-\frac{(k_B T \ln \Omega + H)}{k_B T}}; \quad (15)$$

where Ω is the number of configurations included in each sub-space. The last equality in the above equation can be understood as if each sub-space of the configurational phase space is represented by only one configuration with height function $h(x; y)$ whose energy is given by the sum of Helfrich elastic energy and an extra term that accounts for the "degeneracy" of the corresponding sub-space:

$$H_{\text{sub space}} = k_B T \ln \Omega + \frac{\kappa}{2} \int \nabla^2 h^2 d^2 \mathbf{r}; \quad (16)$$

In the case of a free membrane, the number of configurations in each sub-space is obviously the same: $\Omega = \Omega_0 = (L=l)^2$. (Note that for the purpose of counting the number of configurations, we henceforth assume that two configurations are distinct only if they are shifted by at least one grid cell of microscopic area l^2 with respect to each other.)

Let us repeat the above argument for our model system shown in Fig. 2. In this case, the mapping transformation between configurations belonging to the same sub-space involves two steps: (i) a horizontal translation in the $x-y$ plane, and (ii) a vertical translation in the normal z direction which sets the height of the corners to be $h(0;0) = h(0;L) = h(L;0) = h(L;L) = d$ above the underlying surface (see Fig. 4 (A)). The Helfrich energy is invariant under these transformations. However, the vertical translation may lead to the intersection of the membrane with the surface and, therefore, to the exclusion of the configuration from the sub-space of allowed configurations (Fig. 4 (B)). The number of configurations left in each sub-space $\Omega = \Omega_0 G(h(x;y);d)$. Introducing the function $G(h(x;y);d) \leq 1$, we can write $\Omega = \Omega_0 G(h(x;y);d)$ and rewrite Eq.(16)

$$H_{\text{sub-space}} = k_B T \ln \Omega_0 + k_B T \ln G(h(x;y);d) + \frac{1}{2} \int_0^L r^2 h^2 d^2 x; \quad (17)$$

Adding the term $+ k_B T \ln \Omega_0$ to Eq.(17) allows us to replace the summation over "sub-spaces" back with summation over all the possible configurations of a "free" membrane (without a surface). The effective Hamiltonian of this "free" membrane is given by

$$H = k_B T \ln G(h(x;y);d) + \frac{1}{2} \int_0^L r^2 h^2 d^2 x; \quad (18)$$

There is no EV term in this Hamiltonian (since the membrane is assumed to be free), but these interactions between the membrane and the surface are properly accounted for by the first term on the right hand side which quantifies the effect of the surface on the configurational entropy of the membrane.

An interesting and unexpected result can be obtained in the $d = 0$ limit, i.e., when the corners of the membrane are placed directly on the surface. In this limit, the transformation defined between configurations within each sub-space (see Fig. 4 (A)) will almost always generate "forbidden" configurations that intersect the surface (Fig. 4 (B)). Only when the pinning point coincides with the global minimum of $h(x;y)$, then the membrane will be positioned above the surface over the entire frame region. Therefore, each sub-space includes only one configuration: $\Omega = 1$ (neglecting the measure-zero set of configurations with multiple global minima), which means that $G(h(x;y);0) = \Omega_0 = (L=l)^2$ does not depend on $h(x;y)$. Substituting this result into Eq.(18), we find that a constant term was added to the Helfrich energy of the free membrane. Therefore, the statistical mechanical properties of the pinned membrane are identical to those of the free membrane and, in particular, its fluctuation spectrum is also given by Eq.(4).

How can we evaluate the function $G(h(x;y);d)$ defined above? Let us consider again the mapping transformation between configurations belonging to the same configurational sub-space (Fig. 4 (A)). This transformation changes the pinning point by translating the membrane both horizontally and vertically. The number of allowed configurations in the sub-space is determined by the number of points on the membrane which can be placed a height d above the surface without causing any part of the membrane to intersect the surface. The set of such possible pinning points includes all the points on the membrane for which $h(x;y) \leq h_{\min} + d$, where h_{\min} is the global minimum of the height function. These points are located below the dashed horizontal line in Fig. 5. Denoting by $A_p(h(x;y);d) < L^2$ the total projected area associated with this set of possible pinning points, the function $G(h(x;y);d) = A_p/L^2$ represents the fraction of membrane points that satisfy the "pinning condition" $h(x;y) \leq h_{\min} + d$.

Let us introduce the height distribution function of the membrane, $p_h(x;y)(z)$. For a given height function $h(x;y)$, $p_h(x;y)(z)dz$ gives the fraction of membrane points for which $z < h(x;y) < z + dz$. The function $G(h(x;y);d)$ is the cumulative distribution function associated with $p_h(x;y)(z)$:

$$G(h(x;y);d) = \int_{h_{\min}}^{h_{\min} + d} p_h(x;y)(z) dz; \quad (19)$$

We proceed by approximating $p_h(x;y)(z)$ by a Gaussian distribution function [26]

$$p_h(x;y)(z) = \frac{1}{\sqrt{2\pi} \sigma_h(x;y)} \exp \left\{ -\frac{(z - \bar{h})^2}{2\sigma_h^2(x;y)} \right\}; \quad (20)$$

where

$$\sigma_h^2(x;y) = \overline{(h - \bar{h})^2} = \frac{1}{L^2} \sum_{q \in 0}^4 h_q^2; \quad (21)$$

Using Eq.(20) in Eq.(19), we find :

$$G(h(x,y);d) = \frac{1}{2} \left[1 + \operatorname{erf} \left(\frac{h_{\text{in}} - h + d}{\sqrt{2} h(x,y)} \right) \right] = \frac{1}{2} \left[1 + \operatorname{erf} \left(\frac{d}{\sqrt{2} h(x,y)} \right) \right]; \quad (22)$$

where $\operatorname{erf}(x) = \frac{2}{\sqrt{\pi}} \int_0^x e^{-u^2} du$ is the standard error function, and $h_{\text{in}} - h = \sqrt{2} h(x,y) > 0$. The function $G(h(x,y);d)$ given by Eq.(22) satisfies the boundary condition that $G(d \rightarrow 1) \rightarrow 1$. The value of d can be set by imposing the other boundary condition (see discussion above) that $G(d=0) = (L/L)^2$, which gives

$$d = \sqrt{2} h(x,y) \operatorname{erf}^{-1} \left(1 - \frac{L^2}{L^2} \right); \quad (23)$$

Using the Fourier representation fh_q of the function $h(x,y)$ and Eqs. (18) and (22), we find that the statistical mechanical properties of the pinned membrane can be derived by considering a free membrane whose thermal behavior is governed by the Hamiltonian:

$$H = k_B T \ln \left[\frac{1}{2} + \frac{1}{2} \operatorname{erf} \left(\frac{d}{\sqrt{2} h(x,y)} \right) \right] + \frac{L^4}{L^2} \sum_q \frac{q^4}{2} h_q^2; \quad (24)$$

where d is given by Eq.(23). The dependence of the first term on the right hand side of Eq.(24) on fh_q is contained in the variable $h(x,y)$ (see Eq.(21)). The spectral intensity of the pinned membrane can be calculated by using the equipartition theorem:

$$k_B T = h_q \frac{\partial H}{\partial h_q} \quad (25)$$

Introducing the variable $d = \sqrt{2} h(x,y) \operatorname{erf}^{-1} \left(1 - \frac{L^2}{L^2} \right)$, the right hand side of Eq.(25) can be written as follows:

$$\begin{aligned} h_q \frac{\partial H}{\partial h_q} &= \frac{L^4}{L^2} q^4 h_q^2 - k_B T \frac{2}{\sqrt{2} h(x,y)} \frac{\partial d}{\partial h_q} h_q \\ &= \frac{L^4}{L^2} q^4 h_q^2 + k_B T \frac{2}{\sqrt{2} h(x,y)} \frac{\partial d}{\partial h_q} h_q \\ &= \frac{L^4}{L^2} q^4 + k_B T \frac{d}{\sqrt{2} h(x,y) L^2} \frac{\partial d}{\partial h_q} h_q^2; \end{aligned} \quad (26)$$

Eq.(26) represents a set of linear equations (one for each Fourier mode $q \neq 0$). These equations are coupled to each other through the mean-square height fluctuation $h(x,y)$ (see Eq.(21)) appearing both explicitly on the second term in the curly brackets, as well as in the definition of the variable d . For both $d \rightarrow 1$ (free membrane) and $d = 0$ (membrane pinned directly to the surface) the second term in the curly brackets vanishes and, therefore, Eq.(4) which describes the fluctuation spectrum of a free membrane is recovered in these two limits, as argued above. For finite values of d , a further approximation can be made by replacing the spatial average $h(x,y)$ with h_0 , the ensemble average over free membrane configurations (see Eq.(5)). This approximation leads to the decoupling of the set of equations (26) and yields the following result:

$$h_q^2 = \frac{k_B T L^2}{L^4 q^4 + k_B T \frac{d}{\sqrt{2} h_0 L^2} \frac{\partial d}{\partial h_q} h_q^2}; \quad (27)$$

where within the approximation of replacing $h(x,y)$ with h_0 , we also set $d = \sqrt{2} h_0 \operatorname{erf}^{-1} \left(1 - \frac{L^2}{L^2} \right)$. Eq.(27) has the same form as Eq.(8) which describes the power spectrum of a membrane fluctuating under the action of a uniform harmonic potential of strength

$$e = k_B T \frac{d}{\sqrt{2} h_0 L^2} \frac{\partial}{\partial h_q} \left[\frac{e^{-\left(\frac{d}{\sqrt{2} h_0} \right)^2}}{1 + \operatorname{erf} \left(\frac{d}{\sqrt{2} h_0} \right)} \right]; \quad (28)$$

From Eq.(27) we conclude that the thermal height fluctuations of the pinned membrane are attenuated compared to the fluctuations of a free membrane. The mean square fluctuation amplitude of a mode with wavevector $q = 2\pi n/L$ is reduced by a factor

$$I_n = \frac{\langle h_{q(e)}^2 \rangle}{\langle h_{q(e=0)}^2 \rangle} = \frac{q^4}{q^4 + \frac{e}{L^4}} = \frac{n^4}{n^4 + n^4}; \quad (29)$$

where

$$n^4 = \frac{e}{L^4} = \frac{k_B T}{(2\pi)^4} \frac{dL^2}{0} \exp \left[-\frac{r}{2} \frac{e \left(1 + \frac{d}{2} \right)^2}{1 + \operatorname{erf} \left(\frac{d}{2} \right)} \right] \quad (30)$$

is a dimensionless number that governs the crossover between the regimes of damped ($n^4 \ll n^4$) and free ($n^4 \gg n^4$) thermal fluctuations. Values of n^4 are plotted in Fig. 6 for different values of d and for $\beta = 10k_B T$ and $L = 101.50 \text{ nm}$ ($\beta = 1.645$ – see Eq.(23)). The maximum value of $n^4 = 0.34$ is obtained for $d = 0.025 - 0.04L = 1.25 - 2 \text{ nm}$. This value of $n^4 = 0.34$ is too small to have any noticeable effect on the spectrum of thermal fluctuations, except for the largest mode ($n = 1$) whose square amplitude is suppressed by a factor of $I_1 = 1.34 = 0.75$. In comparison, the square amplitudes of second and third largest modes are reduced by only factors of $I_2 = 0.92$ and $I_3 = 0.98$, respectively. We also observe from Fig. 6 that for smaller values of β , the maximum values of n occurs at larger values of $d=L$. This behavior is anticipated since the smaller β the larger the amplitude of the thermal fluctuations and, therefore, the greater the range of steric repulsion between the membrane and the surface. However, even for very soft membranes with $\beta = 3k_B T$, the maximum is still reached at $d=L < 0.1$, i.e., only a few nanometers above the surface.

III. COMPUTER SIMULATIONS

One of the important recent advances in soft-matter simulations is the development of coarse-grained (CG) bilayer membrane models in which the membranes are simulated without direct representation of the embedding solvent [27, 28]. These implicit solvent ("solvent free") CG models require modest CPU and memory resources and, therefore, can be used for simulations of mesoscopically large membranes over long enough timescales to address experimental reality. Here, we use an implicit solvent CG model to test the validity and accuracy of the analytical predictions discussed above. A snapshot from the simulations is shown in Fig. 7. Each lipid molecule is represented by a short string of three spherical beads of diameter σ , where one of the beads (depicted as a dark gray sphere in Fig. 7) represents the hydrophilic head group and two beads (light gray spheres in Fig. 7) represent the hydrophobic tail of the lipid. The details of the model and of the molecular simulations are given in refs. [29] and [30], including the description of a new Monte Carlo scheme (Mode Excitation Monte Carlo) which has been applied to accelerate the relaxation of the p largest Fourier modes corresponding to $n = 1; \frac{p}{2}; \frac{p}{5}; \frac{p}{8}$. The simulated system consists of a bilayer membrane of 2000 lipids and a surface (whose boundary is indicated by a thick black line) located at $z = 0$ below which the beads cannot be found. The center of the head bead of one of the lipids in the lower leaflet (indicated by a black sphere appearing at the front of Fig 7) is held fixed at $\mathbf{r} = (x; y; z) = (0; 0; d + \frac{\sigma}{2})$. Note that in our simulations, d is defined as the distance between the surface and the bottom of the particle whose position is held fixed. The simulations were carried out on the "high performance on demand computing cluster" at Ben Gurion University. For each value of d , the simulation results appearing below are based on 16 independent runs, each of 1.2×10^6 Monte Carlo time units. The first 2×10^5 time units of each run were discarded from the statistical analysis.

The simulations were conducted in the constant surface tension ensemble, at vanishing surface tension. We set the bead diameter, $\sigma = 6 \text{ nm}$, so that the bilayer membrane thickness is $l = 6 \times 5 \text{ nm}$, and the (mean) linear size of the bilayer $L = (36.4 \pm 0.1) \times 30 \text{ nm}$ (for all values of d). The spectrum of the membrane height fluctuations $\langle h_{q(e)}^2 \rangle$ is plotted in Fig. 8 for both $d = 0$ and $d = 1$ (i.e., for a freely fluctuating membrane). The computational results fully confirm our analytical prediction that the power spectra in these two cases are identical. By fitting the computational results to the asymptotic form (for small values of n) Eq. (4), we obtain that the bending rigidity of the membrane $\kappa = (7.8 \pm 0.2) k_B T$.

For $d \neq 0$ we expect the power spectrum of the membrane to be "almost" identical to the power spectrum of the free membrane. More precisely, Eq. (29) predicts that the mean square fluctuation amplitudes of the modes will be reduced by a factor I_n which, except for the longest $n = 1$ mode, is very close to unity. This prediction is very well supported by our computational results which are summarized in Table I. The table gives the values I_1 and I_2 (corresponding, respectively, to the largest and second largest Fourier modes) for different values of d . Within the

statistical accuracy of our simulation results, we found no change in the fluctuation amplitudes of all the other modes corresponding to wavenumbers $n \geq 2$. In order to evaluate the quantitative agreement between the computational data presented in Table I and the above analytical theory, we use Eqs. (5), (23), (29), and (30) to calculate the factor I_1 for different values of d and for the set of parameters relevant to our simulations: $\beta = 7.8 k_B T$, $L = 6l = 36$. The results of the calculation along with our computational results (Table I) are plotted in Fig. 9. As can clearly be seen in the figure, the agreement between the analytical and computational results is quite good. This agreement lends support for the validity and accuracy of our theoretical analysis of the fluctuation spectrum.

IV. THE DISJOINING PRESSURE

The fact that surface influence on the bilayer fluctuations can be effectively described in terms of a uniform harmonic potential, does not imply that the disjoining pressure between the surface and the membrane follows Eq.(13). The pressure can be related to Hamiltonian (24) through the following equation:

$$p = -\frac{1}{L^2} \frac{\partial H}{\partial d}; \quad (31)$$

from which we readily derive that

$$p = \frac{k_B T}{L^2} \int_0^L \int_0^L \frac{1}{h(x,y)} \frac{e^{-\left(\frac{d}{2h(x,y)}\right)^2}}{1 + \operatorname{erf}\left(\frac{d}{2h(x,y)}\right)} dx dy \quad (32)$$

Following the approach described in section II, the thermal average in Eq.(32) can be approximately evaluated by replacing $h(x,y)$ with h_0 (Eq.(5)), which gives the following expression:

$$p = \frac{k_B T}{L^2} \int_0^L \int_0^L \frac{1}{h_0} \frac{e^{-\left(\frac{d}{2h_0}\right)^2}}{1 + \operatorname{erf}\left(\frac{d}{2h_0}\right)} dx dy = p_H(d); \quad (33)$$

where $p = (k_B T)^{1/2} L^3$, $d = \frac{d}{h_0}$, and $C = (2)^2 (2\sqrt{3})^{1/2} = 12\sqrt{3}$. The scaling function $H(d)$, which is plotted in Fig. 10, decreases monotonically with d . At large distances ($d \gg 1$) the pressure decreases as $\exp[-(d/L)^2]$. The maximum pressure occurs when the membrane is in direct contact with the surface ($d = 0$). The contact pressure, however, does not diverge but rather reaches the following finite value $p(d=0) = p_H(0) = p_H^C$. Using Eqs. (23) and (33), one can easily realize the contact pressure diminishes with the size of the membrane patch:

$$p(d=0) = p_H^C = \frac{p}{L^3} \ln \frac{L}{1} \quad (34)$$

V. CONCLUDING REMARKS

In this paper, we analyzed the influence of EV volume effects on the statistical mechanical properties of supported membranes. Using analytical calculations and Monte Carlo simulations, we determined the fluctuation spectrum of a bilayer membrane patch of a few tens of nanometer in size whose corners are located at a fixed distance d above a plane rigid surface. We found that the surface has influence on the fluctuation spectrum of the membrane only when the pinning distance d is sufficiently small ($d \leq L$ - see Figs. 6 and 9). This result can be easily understood given the fact that the amplitude of the height fluctuations of a free membrane patch satisfies $h_0 \approx 0.02L$ (see Eq. 5)) and, obviously, the membrane hardly collides with the underlying surface when $d \gg h_0$. At small distances ($d \ll h_0$), the surface influence on the bilayer fluctuation spectrum resembles that of a uniform harmonic confining potential of the form: $V = (l/2) \epsilon(d)h^2$. Both analytically and computationally we find that the strength $\epsilon(d)$ of the effective harmonic potential is extremely small and has noticeable impact only on the amplitudes of the very largest fluctuation modes. More remarkably, the confinement effect vanishes ($\epsilon(d) = 0$), when the membrane is brought into direct contact with the surface ($d = 0$). This unexpected and counterintuitive result can be explained by the fact that the thermal motion of the membrane is not really confined within a finite spatial region (as in a stack of bilayer membranes) but only restricted on one side. Therefore, the primary effect of the collisions with the underlying surface

is to push the membrane "upward" rather than to suppress the amplitude of the fluctuations. This is also the reason why the disjoining pressure does not diverge when d vanishes.

The significance of our findings should be considered in light of previous theoretical attempts to quantify the steric effects between membranes and underlying supported interfaces. Some of these studies describe the wall-membrane pressure by means of Eq.(13), which we have shown to be irrelevant for this problem. One particular problem that should be reanalyzed in light of our new results is the theoretical interpretation of the fluctuation spectra of red blood cells [31]. The plasma membrane of red blood cells is attached to a triangulated network of flexible spectrin proteins with mesh size $\approx 60-100$ nm. The spectrum of red blood cells fluctuations was analyzed in terms of the Helfrich-Hamiltonian with both curvature and scale dependent surface tension terms, where the latter term originates from the coupling to the cytoskeleton. Using a Gaussian network model, Fournier et al. [17, 18] showed that the effective surface tension exhibits a steep crossover from a vanishingly small value at length scales smaller than ≈ 100 nm to some finite value at scales larger than ≈ 100 nm. Gov et al. [16, 21] argued that, in addition, a uniform harmonic potential term must be introduced in the Helfrich effective surface Hamiltonian, which accounts for the conformational entropic effect due to the steric repulsion between the spectrin and the bilayer. Our statistical mechanical analysis partially supports this phenomenological argument. On the one hand, our Eq.(27) can be interpreted in terms of a uniform harmonic potential that acts on the membrane. On the other hand, our estimation of the strength of the effective harmonic potential makes it questionable whether the origin of it can be attributed to EV interactions (between the bilayer and the spectrin) alone. It seems more likely to relate this additional conformational entropic term to the junctional complexes (of short actin filaments, globular band 4.1, and other proteins) which connect the membrane to the cytoskeleton and restrict the membrane height fluctuations around the points of attachment. We thus speculate that, just like the surface tension, the strength of the effective harmonic potential ϵ must also be scale dependent. At length scales below the mesh size, we expect the value of ϵ to be governed by EV effects and, therefore, to be extremely small. Above the mesh size, the strength of the harmonic conformational entropic will be determined by the strength of the periodic pinning of the membrane to the cytoskeleton which, presumably, result in a larger value of ϵ . It should be stressed here that there is currently no proof (or even a reasoned argument) that the long wavelength fluctuations of red cells are indeed harmonically confined. One should also bear in mind that on the scale of the mesh size of the network, the problem is quite intricate and issues such as connectivity defects and the motion of the protein anchors must be properly addressed.

Discussions with Nir Gov, Thorsten Auth, Sam Safran and Phil Pincus are gratefully acknowledged.

-
- [1] Handbook of Biological Physics: Structure and Dynamics of Membranes edited by R. Lipowsky and E. Sackmann (Elsevier, Amsterdam, 1995).
 - [2] B. Alberts, D. Bray, J. Lewis, M. Raff, K. Roberts, and J.D. Watson, Molecular Biology of the Cell (Garland, New York, 1994).
 - [3] T. Salaita, J. Phys.: Condens. Matter 17, R287 (2005).
 - [4] M. Tanaka and E. Sackmann, Nature 437, 656 (2005).
 - [5] M. Tanaka and E. Sackmann, Phys. Stat. Sol. (a) 203, 3452 (2006).
 - [6] P.P. Girard, E.A. Cavalcanti-Adam, R. Kemmerer, and J.P. Spatz, Soft Matter 3, 307 (2007).
 - [7] J. Salafsky, J.T. Groves, and S.G. Boxer, Biochemistry 35, 14773 (1996).
 - [8] J. Salafsky, J.T. Groves, and S.G. Boxer, Science 271, 5245 (1996).
 - [9] S. Daniel, F. Albertorio, and P.S. Cremer, MRS Bull. 31, 536 (2006).
 - [10] P.S. Swain and D. Andelman, Phys. Rev. E 63, 051911 (2001).
 - [11] K.R. Mecke, T. Charitat, and F. Graner, Langmuir 19, 2080 (2003).
 - [12] L.C.-L. Lin and F.L.H. Brown, Phys. Rev. Lett. 93, 256001 (2004).
 - [13] L.C.-L. Lin, G.T. Groves, and F.L.H. Brown, Biophys. J. 91, 3600 (2006).
 - [14] R.-J. Merath and U. Seifert, Phys. Rev. E 73, 010401(R) (2006).
 - [15] R.-J. Merath and U. Seifert, Eur. Phys. J. E 23, 103 (2007).
 - [16] N. Gov, A.G. Zilman, and S. Safran, Phys. Rev. Lett. 90, 228101 (2003).
 - [17] J.-B. Fournier, D. Lacoste, and E. Raphael, Phys. Rev. Lett. 92, 018102 (2004).
 - [18] C. Dubus and J.-B. Fournier, Europhys. Lett. 75, 181 (2006).
 - [19] T. Auth, S.A. Safran, and N.S. Gov, Phys. Rev. E 76, 051910 (2007).
 - [20] R. Zhang and F.L.H. Brown, J. Chem. Phys. 129, 065101 (2008).
 - [21] N. Gov and S.A. Safran, Phys. Rev. E 69, 011101 (2004).
 - [22] R. Bruinsma, M. Gullian, and P. Pincus, Biophys. J. 67, 746 (1994).
 - [23] W. Helfrich, Z. Naturforsch. 33a, 305 (1978).
 - [24] R. Lipowsky, in ref. [1].
 - [25] S. Safran, Statistical Thermodynamics of Surfaces, Interfaces, and Membranes (Addison-Wesley, New York, 1994).
 - [26] Strictly speaking, the fluctuations behavior of fluid membranes differs from that of random surfaces even on macroscopically

length scales. Therefore, the validity of Eq.(20) cannot be rigorously justified. The good agreement of the results [Eq.(27)] with the computer simulations gives credibility to this approximation. The Gaussian form becomes exact if the membrane is subjected to a strong pinning potential of localized harmonic springs, see: L.C.-L. Lin and F.L.H. Brown, Biophys. J. 86, 764 (2004).

- [27] O. Farago, J. Chem. Phys. 119, 596 (2003).
- [28] G. Bannigan, L.C.-L. Lin and F.L.H. Brown, Eur. Biophys. J. 35, 104 (2006).
- [29] I.R. Cooke, K. Kremer, and M. Deserno, Phys. Rev. E. 72, 011506 (2005).
- [30] O. Farago, J. Chem. Phys. 128, 184105 (2008)
- [31] A. Zilker, H. Engelhardt, and E. Sackmann, J. Physique. 48, 2139 (1987).

d	I_1	I_2
0.5	0.89 (5)	0.99 (4)
	0.87 (6)	0.97 (4)
1.5	0.84 (4)	0.94 (4)
2	0.85 (4)	0.95 (4)
2.5	0.90 (6)	0.96 (4)
3.5	0.94 (4)	0.99 (4)
4.5	1.00 (5)	1.00 (4)

TABLE I: The factors I_1 and I_2 (see Eq.(29)) by which the mean square fluctuation amplitudes of the largest ($n = 1$) and second largest ($n = 2$) modes are reduced as compared to the square fluctuation amplitudes of a free membrane. The height d denotes the distance between the bottom of the fixed spherical bead and the underlying surface.

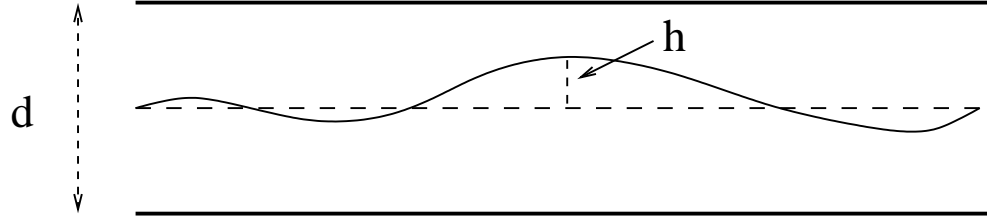


FIG. 1: A fluctuating membrane confined between two walls which are separated from each other by a distance d . The height of the fluctuating membrane, h , is measured from the mid plane between the walls ($d=2h + d=2$).

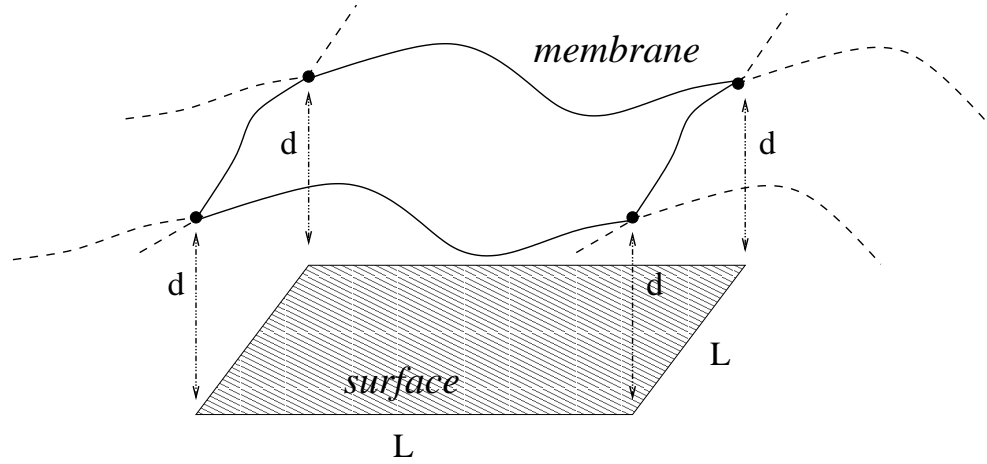


FIG. 2: A square membrane fluctuating above a flat, impenetrable, surface. The function $h(x;y)$ denotes the height of the membrane above the underlying surface. At the four corners of the surface $h(0;0) = h(0;L) = h(L;0) = h(L;L) = d$. Outside the frame region, $h(x;y)$ is defined by periodic extension.

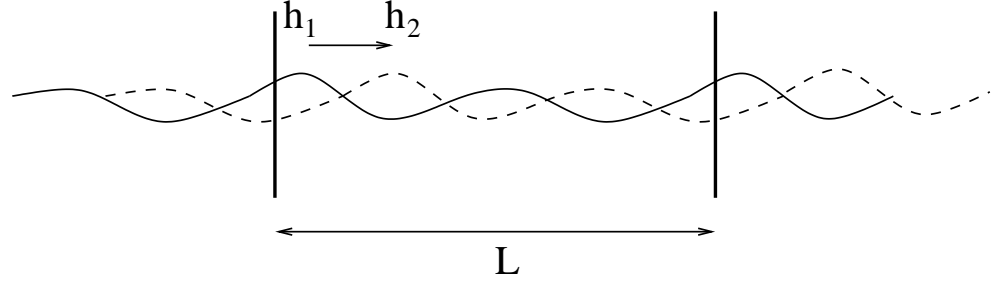


FIG . 3: Configurations that are represented by the height functions $h_1(x;y)$ (solid curve) and $h_2(x;y)$ (dashed curve) belong to the same sub-space of configurations if these configurations are invariant under translation in the x - y plane, i.e., $h_1(x;y) = h_2(x+a;y+b)$ with $0 < a;b < L$.

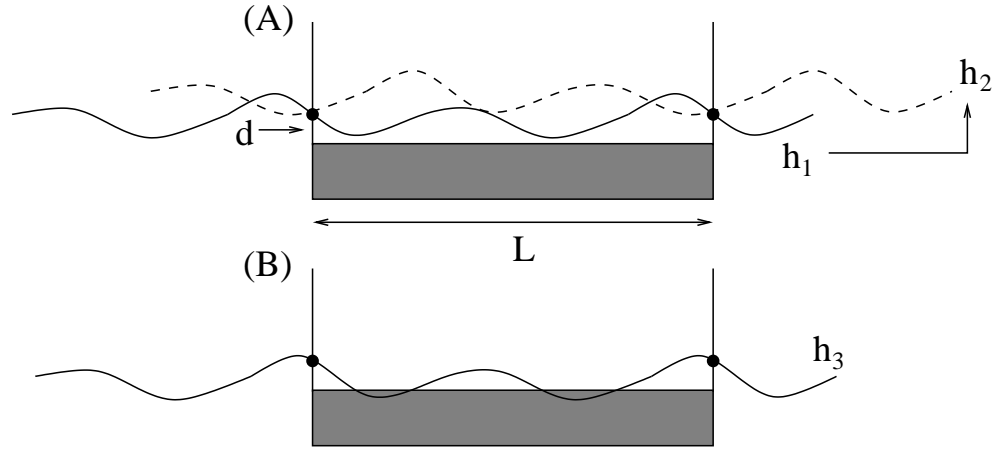


FIG . 4: (A) The transformation between the configurations represented by the height functions $h_1(x;y)$ and $h_2(x;y)$ involves (i) a horizontal translation in the x - y plane and (ii) a vertical translation in the normal z direction that sets the corner at $h_1(0;0) = h_2(0;0) = d$. (B) Configurations such as the one represented by the function h_3 intersect the underlying surface and, therefore, should be excluded from the phase space.

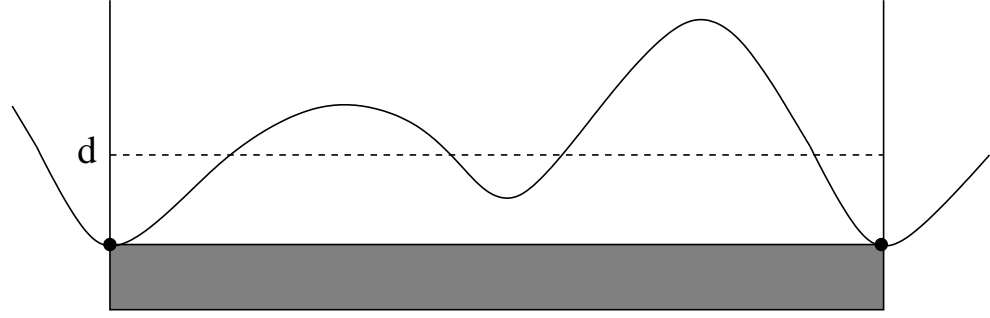


FIG . 5: The membrane can be pinned to the surface without intersecting it only at points for which $h(x; y) > h_{\min} > d$, i.e., the membrane points located below the horizontal dashed line in the figure. Specially, for $d = 0$ the only possible pinning point is at the global minimum of the function h .

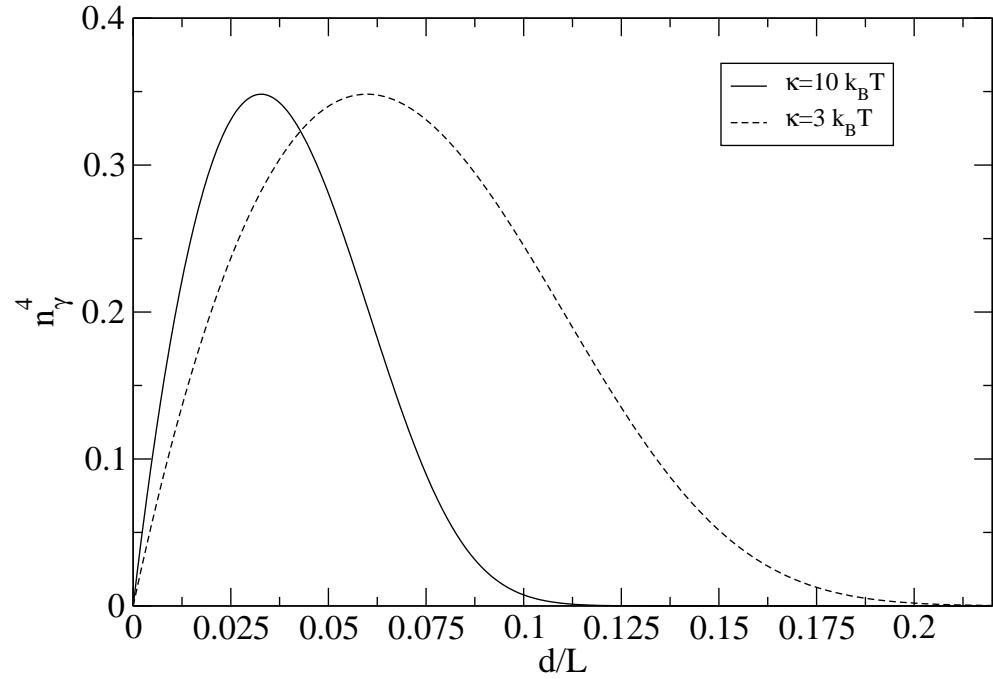


FIG . 6: The dimensionless parameter n^4 (see definition in text -Eq.30) as a function of the height of the pinning points from the surface. The values have been calculated for a membrane of linear size $L = 101$ with bending rigidity $\kappa = 10k_B T$ (solid line) and $\kappa = 3k_B T$ (dashed line).

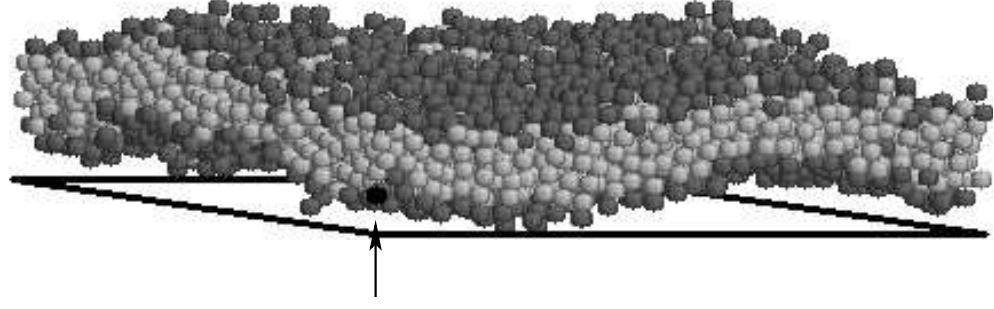


FIG. 7: Equilibrium conformation of a membrane consisting of 2000 lipids. Each lipid is represented by a trimer of one "hydrophilic" bead (dark gray sphere) and two "hydrophobic" beads (light gray spheres). The membrane is fluctuating above a plane surface (frame indicated by a thick black line), while the position of the center of one of the hydrophilic beads (appearing at the front of the figure and indicated by the black sphere and an arrow) is fixed at $\mathbf{r} = (x; y; z) = (0; 0; d + 2)$.

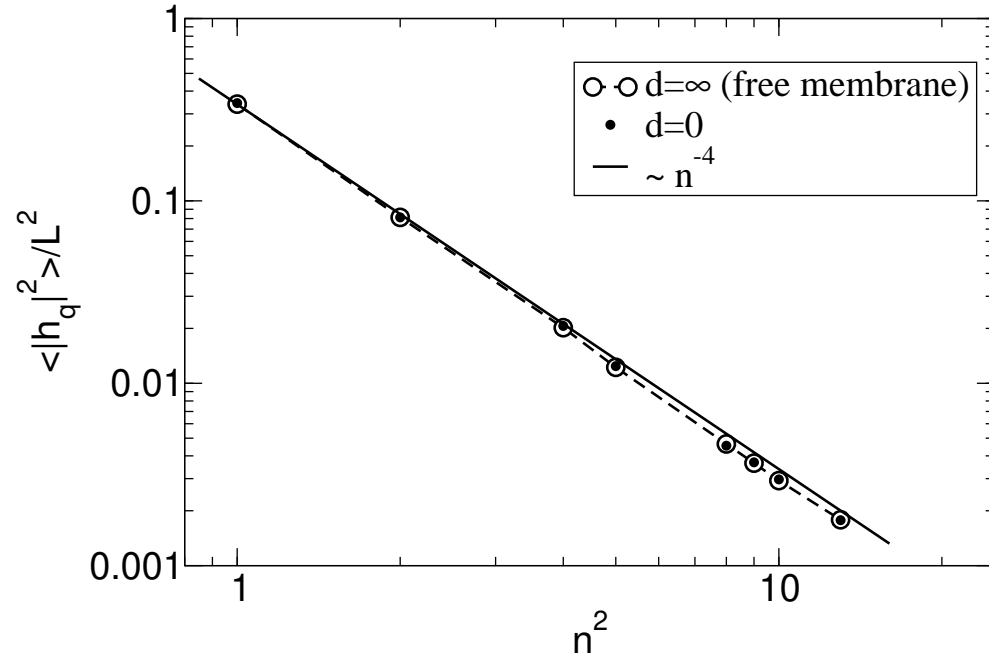


FIG. 8: The fluctuation spectrum of a membrane of $N = 2000$ lipids. The results for $d = 0$ (membrane pinned directly to the surface) are shown by small solid circles. These results are essentially identical to those obtained from simulations of a free membrane ($d = 1$), which are represented by larger open circles connected with a dashed line. The solid line indicates the asymptotic $\langle |h_q|^2 \rangle \sim n^{-4}$ power law.

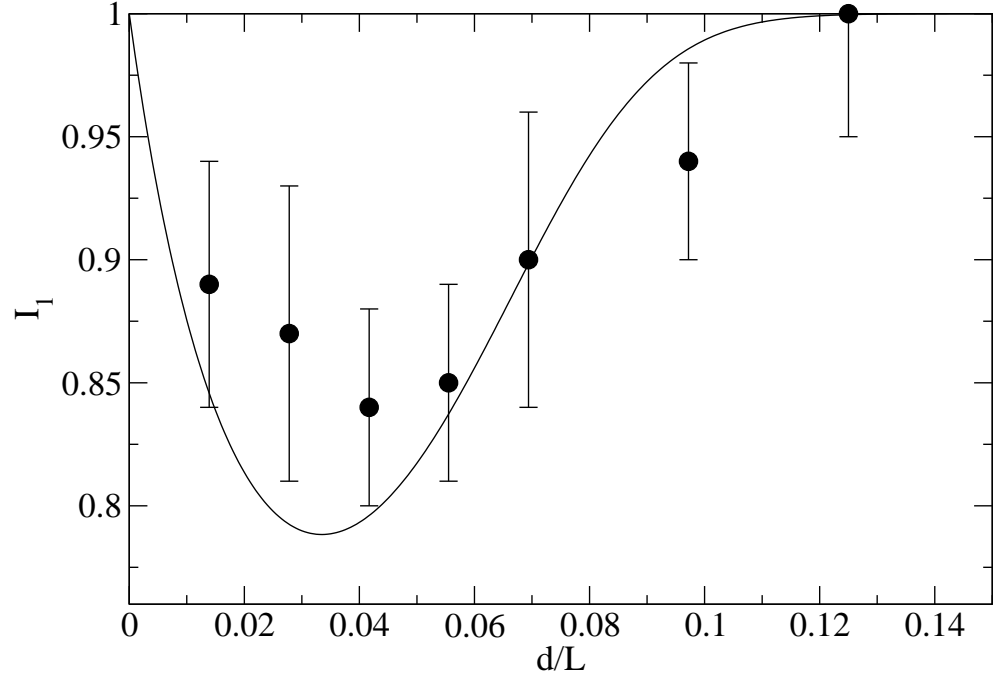


FIG . 9: The factor I_1 as a function of d . Solid circles - computational results (see also Table I). Solid line - analytical results for the computationally relevant parameters: $L = 6l$ and $\beta = 7.8k_B T$.

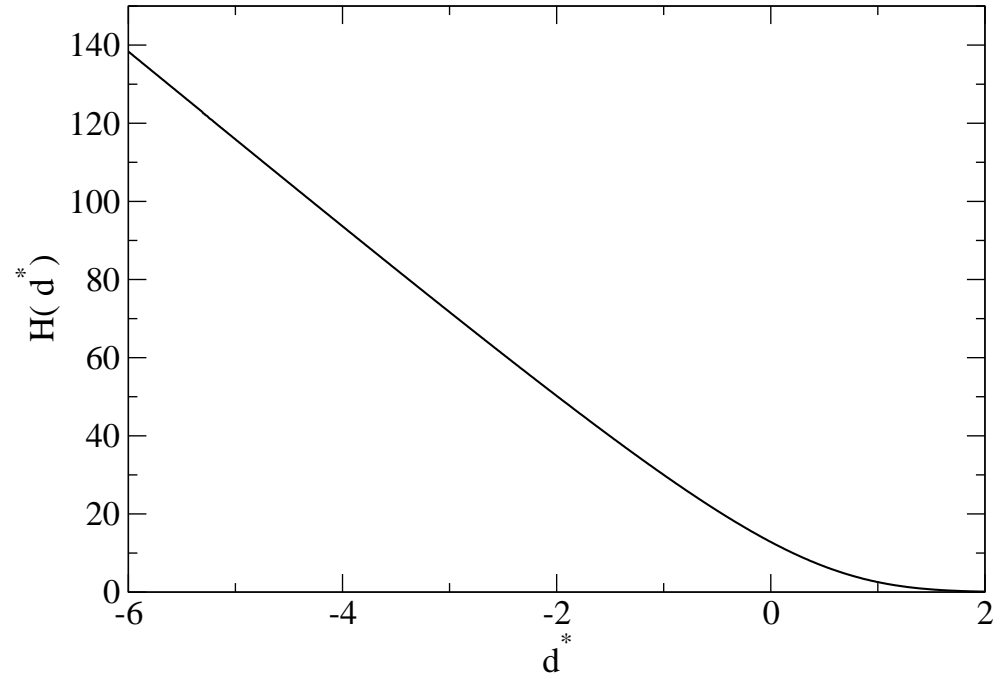


FIG . 10: The scaling function $H(d^*)$ (see definition - Eq.(33)).